Sustainable Energy & Fuels

COMMUNICATION

View Article Online
View Journal | View Issue

Open Access Article. Published on 03 maj 2018. Downloaded on 2026-05-13 17:43:32.
This article is licensed under a Creative Commons Attribution 3.0 Unported Licence.

Check for updates

Cite this: *Sustainable Energy Fuels*, 2018, **2**, 1446

Received 6th March 2018
Accepted 27th April 2018

DOI: 10.1039/c8se00110c

rsc.li/sustainable-energy

Poly(ionic liquid) binders as ionic conductors and polymer electrolyte interfaces for enhanced electrochemical performance of water splitting electrodes†

Ioannis Spanos,[b] Sebastian Neugebauer,[b] Ryan Guterman,[a] Jiayin Yuan,[a] Robert Schlögl[b] and Markus Antonietti *[a]

A poly(ionic liquid) (PIL) was used as a binder for NiCo oxide nanopowder in a water electrolysis standard assay to explore the role of polymers in a model electrocatalytic device. The comparison to technical standard binders such as Nafion™ or Fumion™ ionomers showed that the PIL improves the cycling stability under accelerated ageing conditions as well as the activity.

Electrochemical energy storage and conversion processes are attracting tremendous attention due to their active role in utilizing the fluctuating sources of sustainable energy.[1] New electrode materials and potentially stable solvents and electrolytes have to be developed to survive harsh conditions in electrolysers, fuel cells, and batteries. Interestingly, the binder, needed for the engineering of powder catalysts, is hardly considered to be an object of improvement. Such binder material accounts for typically 10 wt% of the electrode mass and effectively "glues" all powderous components, such as electrochemically active species and conductive additives, into a mechanically stable electrode to endure the operating conditions.[2] A few groundbreaking primary studies[3–8] have shown that significant effects of polymer binders on the overall performance of many electrochemical devices can be expected, particularly with respect to the resulting mechanical properties and interactions with electrolytes and active material. Poly (vinylidene fluoride) (PVDF) is a standard choice for organic electrodes in lithium ion batteries, but even for PVDF the lifetime is restricted, as for instance proven by the increase in contact resistance throughout longer operational runs or even just by the detection of degradation products within the devices.[9] For aqueous systems, purely hydrophobic systems have to be avoided, and a standard choice is for instance Nafion™-based binders.[10] From a chemical perspective, Nafion is a well-known ion and water conductive membrane material, but it is not designed to survive both the harsh reductive as well as oxidative conditions in modern electrodes, as it will be also shown below. We believe that next-generation binders must be able to participate in the main electrochemical reactions and be significantly more robust and conductive than the state-of-the-art to solve the issues plaguing current systems. Ionic liquids (ILs) are used in several electrochemical energy storage/conversion devices due to their favorable physical properties such as negligible vapor pressure, high ionic conductivity, chemical inertness and most importantly, a broad electrochemical window.[11–17] Recently, the favorable application profile was extended to poly(ionic liquid)s (PILs), which combine ILs with polymer characters.[18–20] PIL copolymers have already been examined as binders for electrodes of lithium batteries and indeed showed superior performance.[21] When applied as binders in cathodes of lithium ion batteries, a vinylimidazolium-based nanoparticle binder offered not only a higher specific capacity compared to PVDF but also an outstanding long-term electrochemical durability for at least 1000 charge–discharge cycles.[22] These primary experiments, though elucidating the great potential of PILs as binders in electrochemical devices, were, however, still performed in organic solvents and at rather moderate oxidation potentials. In order to design a PIL with binding function, it generally must satisfy certain requirements. First, the binder must be sufficiently insoluble in the electrolyte to prevent the dissolution of the PIL and the loss of binding function. Additionally, the PIL should swell within the electrolyte to help facilitate ion transport and retain some activity of the bound components and finally the PIL should be resistant to the operating conditions or react to form a product that is resistant to degradation. The PIL chosen here satisfies these requirements and is easily synthesized on the tens of grams scale. Herein, we extend this work to much higher oxidation potentials and corrosive alkaline aqueous conditions with oxygen in status nascendi, as they are for instance found in water electrolysis. We use a PIL binder to

[a]*Department of Colloid Chemistry, Max Planck Institute of Colloids and Interfaces, Am Mühlenberg 1, D-14476 Potsdam, Germany. E-mail: office.cc@mpikg.mpg.de*
[b]*Max Planck Institute for Chemical Energy Conversion, Department of Heterogeneous Reactions, Stiftstrasse 34-36, Muelheim an der Ruhr, 45470, Germany*

† Electronic supplementary information (ESI) available. See DOI: 10.1039/c8se00110c

This journal is © The Royal Society of Chemistry 2018

Open Access Article. Published on 03 maj 2018. Downloaded on 2026-05-13 17:43:32.
This article is licensed under a Creative Commons Attribution 3.0 Unported Licence.

fabricate a powdery NiCo mixed oxide electrode and compare it with two commercial standard binders and a blank sample without a binder. Not only good performance and high stability could be proven, but the compound system even surpassed the performance of the pure electrocatalyst as such. PILs are a class of functional polymers featuring a high density of IL species, *i.e.*, one per monomer unit, as well as a multivalent binding power *via* covalent connection of IL species into a polymer backbone. The interest in applying PILs as binder materials in electrochemical devices relies on their broad electrochemical window endorsed by the electrochemically stable IL moieties and enhanced surface activity, two of the key criteria in designing binder materials. The chemical structure of the PIL binder tested in this study is shown in Fig. 1. The PIL is imidazolium-based, with the imidazolium cation attached directly to the polyvinylene backbone and was prepared *via* conventional free radical polymerization of an ionic liquid monomer 1-ethyl-3-vinylimidazolium bromide, followed by an anion exchange reaction of the polymer to replace Br^- with an electrochemically inert anion, bis(trifluoromethane sulfonyl)imide (TFSI). While the as-synthesized PIL would normally contain a bromide counter anion, we chose TFSI to reduce the solubility of the PIL in the electrolyte. Tetrafluoroborate and hexafluorophosphate anions are potential candidates to reduce PIL solubility; however they are known to undergo hydrolysis and were not examined.[23] A titration test using a $AgNO_3$ solution proves the quantitative anion exchange process.

The chemical structure of the polymer was characterized and proven by nuclear magnetic resonance spectroscopy (Fig. S1†). The molecular weight of this polymer was characterized to be 130 kDa by gel permeation chromatography. The activity and stability properties of a commercial $NiCoO_2$ mixed oxide catalyst, adhered on a glassy carbon support with PIL, Nafion and Fumion binders and no binder, were investigated by means of linear sweep voltammetry and chronopotentiometry, respectively. All measurements were conducted in an electrochemical flow cell, described elsewhere[24] in 1 M KOH, with internal resistance (IR)-correction (see the ESI†). All stability and activity measurements, in this work, have been performed under chronopotentiometric mode, by applying constant 10 mA cm^{-2} for 2 h and by linear sweep voltammetry at 1.2–1.7 V_{RHE}. For the entirety of catalyst electrochemical characterization a flow rate of 0.86 ml min^{-1} was used, because it provides a good balance between oxygen gas removal from the catalyst surface and sufficient detection, from the ICP-OES, of the catalyst corrosion products. Lower flow rates are unable to provide reproducible experimental conditions due to excessive oxygen bubble formation at such high current densities. The catalyst used in this work was a commercial $NiCoO_2$ mixed oxide (Sigma Aldrich, 99% metal basis, >150 nm particle size). The catalysts reach their operating state, in which all activity and stability measurements are performed in this work, after a preconditioning step by means of cyclic voltammetry between 1.0 and 1.45 V_{RHE} at a scan rate of 100 mV s^{-1} for 250 cycles (Fig. 2).

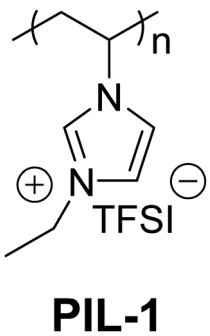

Fig. 1 Chemical structure of the PIL binder tested in this study.

Catalyst activity characterization was performed by means of linear sweep voltammetry between 1.2 and 1.7 V_{RHE} at a scan rate of 5 mV s^{-1} before and after a stability test in chronopotentiometric mode at a current density of 10 mA cm^{-2} for 2 h. The activity gain is observed before and after the preconditioning step. As a result, catalyst preactivation is necessary for the catalyst to reach its final state. Thereafter, linear sweep voltammetry between 1.2 and 1.7 V_{RHE} was applied for a second time on every catalyst to evaluate a comparable catalyst activity (Fig. 3). The catalyst stability was tested using chronopotentiometry at 10 mA cm^{-2} for 2 h (Fig. 4) with simultaneous transient analysis of the corrosion products using an ICP-OES connected to the outlet of the electrochemical flow cell (Fig. 5). After the stability evaluation measurements linear sweep voltammetry was used for the comparison of the initial and final activity of the catalysts investigated. Neither glassy carbon nor the pure PIL binder showed any detectable electrocatalytic water splitting activity as such. NiCo oxide as a bare powder electrode as well as Nafion revealed the same voltage–current-curve, indicating practically resistant-free gluing of the particles. Initially, the PIL binder showed a curve which is shifted to higher potentials by *ca.* 25 mV.

This effect is attributed to a minor amount of added resistance which is more pronounced for Fumion. The catalyst prepared with Nafion presented the highest initial activity among all catalysts. However, upon catalyst preactivation, by cyclic voltammetry, the activity decreased and went down even further after the actual stability test. Similarly, a decrease of the catalytic activity was also observed for the catalyst prepared with Fumion and the binder-free catalyst. In contrast, the catalyst prepared with the PIL-1 binder was significantly activated after the cyclic voltammetry activation step and surprisingly the activity further increased even after the 2 h chronopotentiometric stability investigation (Fig. 3a). This can be attributed to the fast removal of oxygen bubbles from the catalyst surface during the stability tests at a flow rate of 0.86 ml min^{-1} due to the hydrophilic nature of the PIL-1 polymer binder. Fast oxygen bubble accumulation on the catalyst surface reduces the available catalytic surface which results in a fluctuating potential rise observed as spikes recorded in the potential profiles of each catalyst (Fig. 4). Potential spikes have a detrimental effect not only on the catalyst stability but also on the activity. In the case of Fumion the activity was very low ($E_{J=10\ mA\ cm^2} = \sim 2.0\ V_{RHE}$), and the potential during stability measurements was not stable due to inadequate surface oxygen removal. Here, within the first 25 min the oxygen evolution overpotential increased by more

Open Access Article. Published on 03 maj 2018. Downloaded on 2026-05-13 17:43:32.
This article is licensed under a Creative Commons Attribution 3.0 Unported Licence.

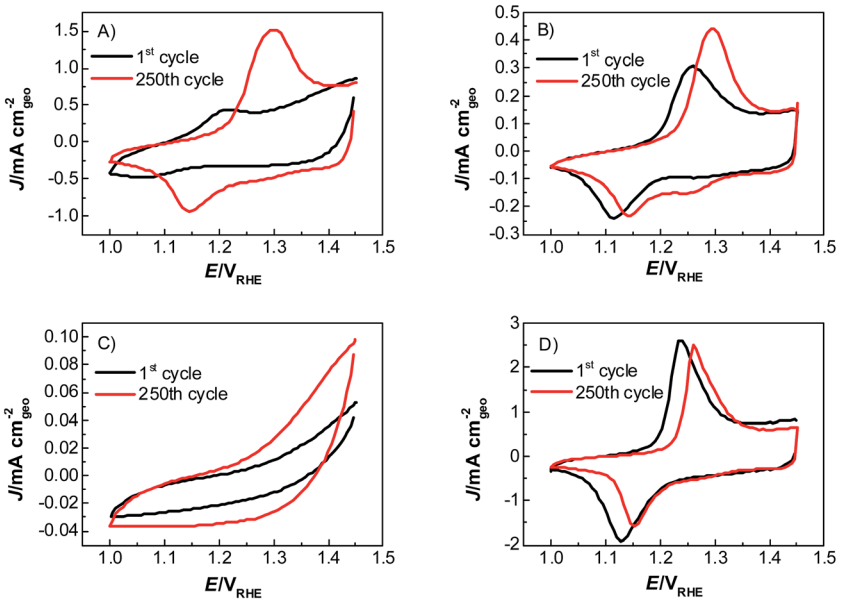

Fig. 2 Cyclic voltammetry between 1.0 and 1.45 V_{RHE} at a scan rate of 100 mV s^{-1} of a mixed $NiCoO_2$ oxide powder catalyst using different binders in 1 M KOH. Significant potential shifts are observed for all catalysts which is evidence of surface ordering. (A and B) PIL-1 and Nafion have a similar potential profile indicating that after potential cycling the catalyst surface remains protected by the binder. (C) The Fumion covered sample is completely inactive due to severe surface coverage by the binder which significantly blocks active sites. (D) The no-binder system shows only a potential shift.

than 100 mV. ICP-OES corrosion profiles follow closely the chrono-potentiometric ones where it could be observed that the potential spikes in the stability measurements and the Ni and Co ICP spikes in the ICP-OES measurements follow a similar pattern due to the higher metal corrosion at higher potential values.

It is known that PILs tend to spread and stick to surfaces of metals[25–27] and some metal oxides,[28] *i.e.*, they try to cover a surface/curved surface with a homogenous film of about 2–5 nm thickness, which also contains solvating water.[29,30] This layer acts as a local membrane, protecting and gluing the catalyst particles, while being permeable to water and anions

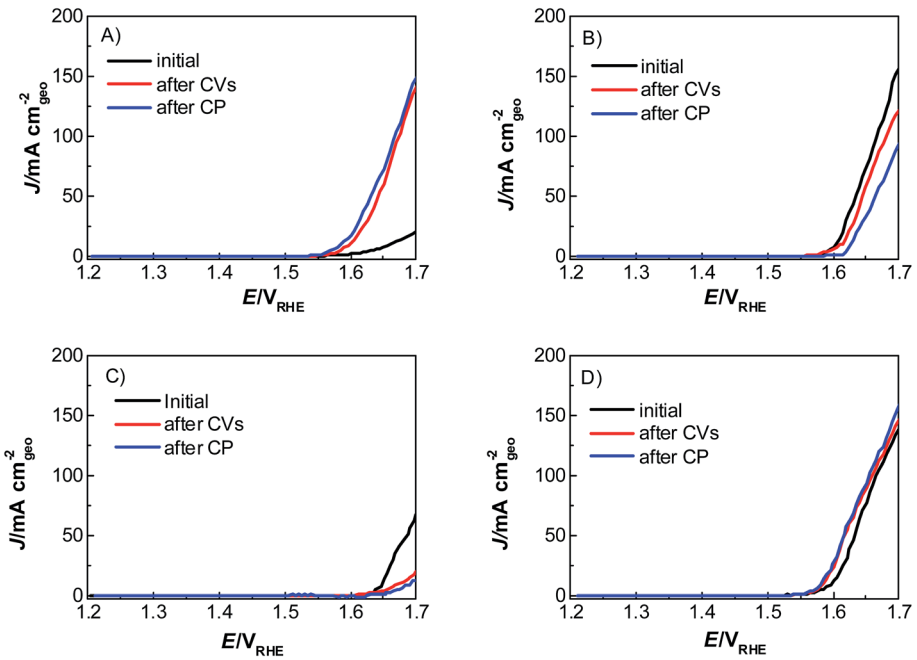

Fig. 3 Linear sweep voltammograms of a commercial mixed oxide $NiCoO_2$ catalyst with (A) PIL-1, (B) Nafion, (C) Fumion and (D) no binder from 1.2 to 1.7 V_{RHE} with a sweep rate of 5 mV s^{-1}, in 1 M KOH.

 This journal is © The Royal Society of Chemistry 2018

Open Access Article. Published on 03 maj 2018. Downloaded on 2026-05-13 17:43:32.
This article is licensed under a Creative Commons Attribution 3.0 Unported Licence.

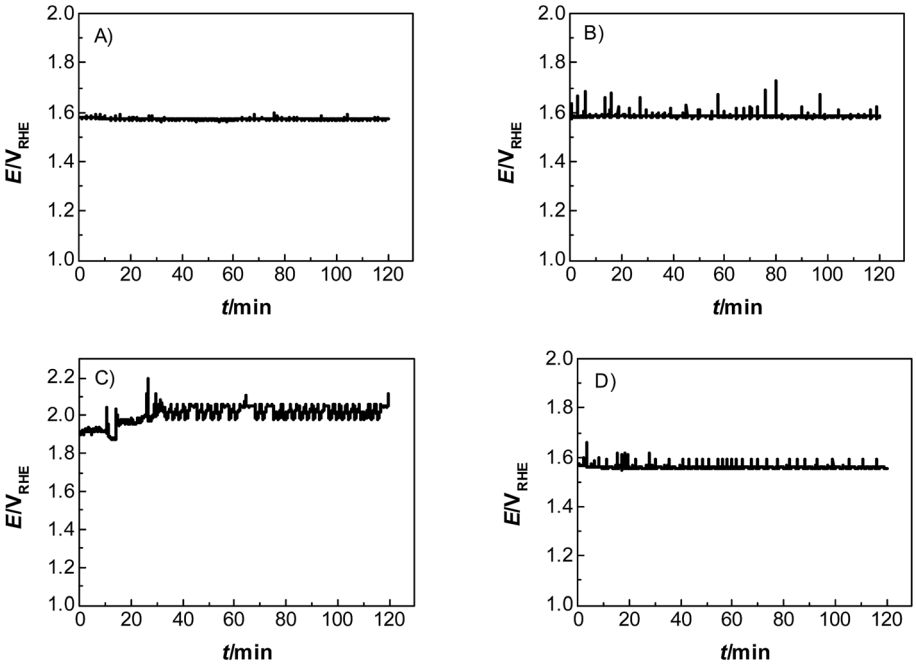

Fig. 4 Chronopotentiometric analysis of the catalyst stability of a commercial mixed oxide $NiCoO_2$ catalyst with (A) PIL-1, (B) Nafion, (C) Fumion and (D) no binder at $j = 10$ mA cm^{-2} for 2 h in 1 M KOH. The catalyst with the Fumion binder shows rather rapid degradation, while the PIL covered catalyst shows similar behavior to the Nafion and no-binder catalysts. However, the increased bubble formation on the Nafion-covered and "no-binder" catalysts can significantly affect the long term stability of the material.

via dynamic counterion exchange. This indicates that the PIL favorably interacts and spreads on the catalyst surface, as opposed to agglomeration which is more typical of an incompatibility. Note that the PIL is a polycation being permeable preliminarily to anions. Unlike some perfluorinated binders, the PIL can swell in the electrolyte and still allows for the activity of the underlying catalyst. Assuming a particle size of 100 nm for the electrocatalyst, we can calculate a stoichiometric layer

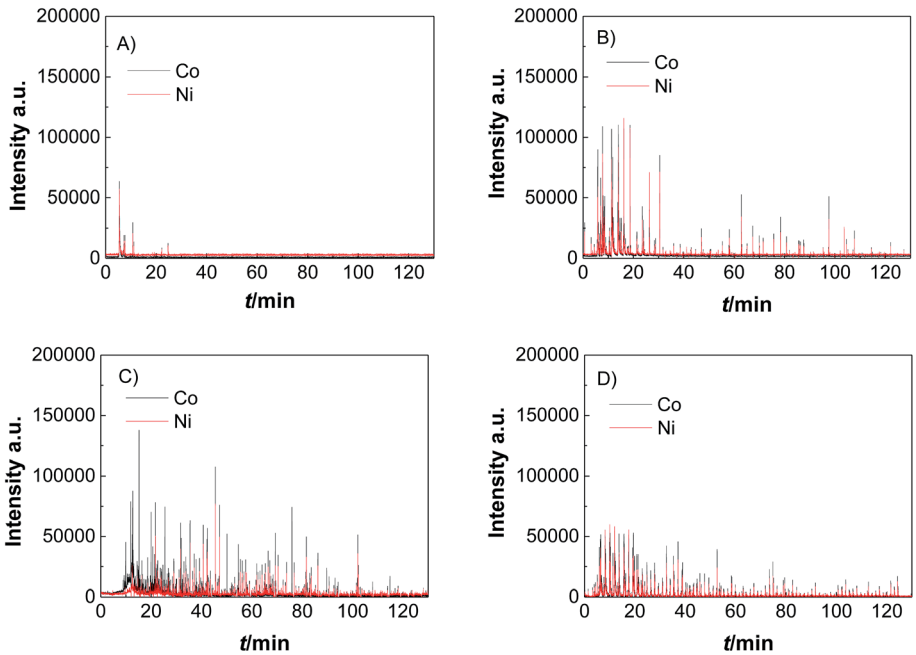

Fig. 5 ICP-OES transient profiles of a commercial mixed oxide $NiCoO_2$ with (A) PIL-1, (B) Nafion, (C) Fumion and (D) no binder in 1 M KOH. Corrosion profiles of each catalyst reveal a significantly better stability for the PIL-1 supported catalyst due to fast oxygen bubble removal from the catalyst surface.

Open Access Article. Published on 03 maj 2018. Downloaded on 2026-05-13 17:43:32.
This article is licensed under a Creative Commons Attribution 3.0 Unported Licence.

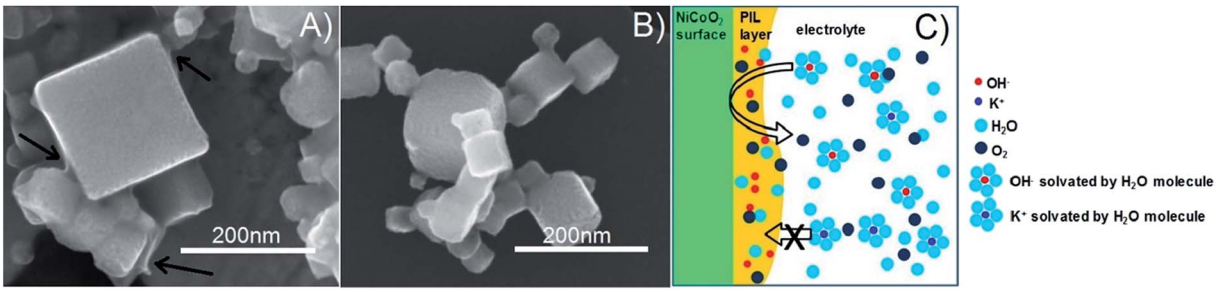

Fig. 6 (A) PIL covered $NiCoO_2$ nanoparticles (arrows in black point at the edges of nanoparticles where the PIL is covering the catalyst), (B) PIL-free nanoparticles and (C) schematic illustration of the PEI. The PIL blocks metals at the electrode, while it is permeable to water, hydroxy ions and the as-generated oxygen, with bubbles nucleating outside the PEI layer.

thickness of *ca.* 5 nm, *i.e.*, there is enough binder available for such a type of distribution. IR-spectroscopy measurements of the catalyst before and after electrochemical measurements revealed that the vibrations corresponding to the PIL remain at ~700 cm^{-1}, ~1200 cm^{-1} and ~1400 cm^{-1}, indicating that the polymer is neither decomposing nor dissolving under experimental conditions. SEM images (Fig. S3†) further prove the existence of the PIL binder before and after the electrochemical stress test at 10 mA cm^{-2}. The fact that the chronoamperometry indicates even an improvement of the electrocatalyst shows that the optimal layer formation and structuration is reached only after 30 minutes of operation, *i.e.*, active SEI formation is a slow process. The destruction of this structure does not occur under the conditions of this test, and for this, we obviously have to move to still higher overpotentials.

Worth mentioning is that the PIL binder outperforms all other systems in terms of peak performance, *i.e.*, the local membrane structure is not at all rate-limiting for the catalytic processes. The whole model is illustrated in Fig. 6.

In conclusion, we show that a polymeric ionic liquid can be used as a binder to formulate nanoparticulate water oxidation catalysts and create a highly active and stable electrode. When compared to two commercial binders, the PIL shows higher oxidation stability and a better lifetime behavior. The addition of the binder even improves the stability of the electrocatalysts as such, which we attribute to the formation of a polymeric solid electrolyte interface layer (PEI), very similar to the solid electrolyte interface layer known from operational batteries, but here not formed *in situ* but *a priori* added. A more realistic stability testing will of course have to include significantly higher overpotentials and potentially other reactions and catalysts. On the other hand, it is still possible to improve the PIL structure to achieve even higher oxidation stabilities, and the related HOMO levels of appropriate organic compounds (to secure thermodynamic stability) can be as positive as +3 V. We believe that the use of functional binders with adjusted swelling, dielectric environment, and ion permeation behavior is a new strategy to impact electrocatalysis and electrochemical heterophase reactions in general, enabling potentially a better rate behavior, but essentially a higher selectivity and longer lifetimes of the resulting overall systems.

Conflicts of interest

There are no conflicts to declare.

Acknowledgements

The authors acknowledge the MAX Planck consortium of MAX-NET Energy and the Max-Planck-Gesellschaft for the support. The authors acknowledge Mr Hans Bongard for the SEM images. Open Access funding provided by the Max Planck Society.

References

1 M. Armand and J. M. Tarascon, *Nature*, 2008, **451**, 652.
2 M. Winter and R. J. Brodd, *Chem. Rev.*, 2004, **104**, 4245.
3 J. Li, R. B. Lewis and J. R. Dahn, *Electrochem. Solid-State Lett.*, 2007, **10**, A17.
4 I. Kovalenko, B. Zdyrko, A. Magasinski, B. Hertzberg, Z. Milicev, R. Burtovyy, I. Luzinov and G. Yushin, *Science*, 2011, **334**, 75.
5 S. Komaba, Y. Matsuura, T. Ishikawa, N. Yabuuchi, W. Murata and S. Kuze, *Electrochem. Commun.*, 2012, **21**, 65.
6 C. V. Amanchukwu, J. R. Harding, Y. Shao-Horn and P. T. Hammond, *Chem. Mater.*, 2014, **27**, 550.
7 M. Wu, X. Xiao, N. Vukmirovic, S. Xun, P. K. Das, X. Song, P. Olalde-Velasco, D. Wang, A. Z. Weber, L.-W. Wang, V. S. Battaglia, W. Yang and G. Liu, *J. Am. Chem. Soc.*, 2013, **135**, 12048.
8 S.-J. Park, H. Zhao, G. Ai, C. Wang, X. Song, N. Yuca, V. S. Battaglia, W. Yang and G. Liu, *J. Am. Chem. Soc.*, 2015, **137**, 2565.
9 S. S. Zhang and T. R. Jow, *J. Power Sources*, 2002, **109**, 422.
10 M. Paidar, V. Fateev and K. Bouzek, *Electrochim. Acta*, 2016, **209**, 737–756.
11 J. Yuan and M. Antonietti, *Polymer*, 2011, **52**, 1469.
12 M. Armand, F. Endres, D. R. MacFarlane, H. Ohno and B. Scrosati, *Nat. Mater.*, 2009, **8**, 621.
13 G. Gebresilassie Eshetu, M. Armand, B. Scrosati and S. Passerini, *Angew. Chem., Int. Ed.*, 2014, **53**, 13342.
14 K. Sakaushi and M. Antonietti, *Bull. Chem. Soc. Jpn.*, 2015, **88**(3), 386.

 This journal is © The Royal Society of Chemistry 2018

Open Access Article. Published on 03 maj 2018. Downloaded on 2026-05-13 17:43:32.
This article is licensed under a Creative Commons Attribution 3.0 Unported Licence.

15 K. Kishimoto, M. Yoshio, T. Mukai, M. Yoshizawa, H. Ohno and T. Kato, *J. Am. Chem. Soc.*, 2003, **125**, 3196.
16 J. Ranke, S. Stolte, R. Störmann, J. Arning and B. Jastorff, *Chem. Rev.*, 2007, **107**, 2183.
17 A. Fernicola, F. Croce, B. Scrosati, T. Watanabe and H. Ohno, *J. Power Sources*, 2007, **174**, 342.
18 J. Yuan and M. Antonietti, *Macromolecules*, 2011, **44**, 744.
19 H. Ohno, *Electrochim. Acta*, 2001, **46**, 1407.
20 G. B. Appetecchi, G. T. Kim, M. Montanino, M. Carewska, R. Marcilla, D. Mecerreyes and I. De Meatza, *J. Power Sources*, 2010, **195**, 3668.
21 J. von Zamory, M. Bedu, S. Fantini, S. Passerini and E. Paillard, *J. Power Sources*, 2013, **240**, 745.
22 J. Yuan, S. Prescher, K. Sakaushi and M. Antonietti, *J. Mater. Chem. A*, 2015, **3**(14), 7229.
23 M. G. Freire, C. M. S. S. Neves, I. M. Marrucho, J. A. P. Coutinho and A. M. Fernandes, *J. Phys. Chem. A*, 2010, **114**(11), 3744–3749.
24 I. Spanos, A. A. Auer, S. Neugebauer, X. Deng, H. Tuysuz and R. Schloegl, *ACS Catal.*, 2017, **7**, 3768.
25 W. Christoph, Y. Jiayin, N. Markus and K. Dorota, *Adv. Funct. Mater.*, 2015, **25**(17), 2537–2542.
26 K. T. Prabhu Charan, N. Pothanagandhi, K. Vijayakrishna, A. Sivaramakrishna, D. Mecerreyes and B. Sreedhar, *Eur. Polym. J.*, 2014, **60**, 114–122.
27 B. Uhl, H. Huang, D. Alwast, F. Buchner and R. J. Behm, *Phys. Chem. Chem. Phys.*, 2015, **17**(37), 23816–23832.
28 M. Wagstaffe, M. J. Jackman, K. L. Syres, A. Generalov and A. G. Thomas, *ChemPhysChem*, 2016, **17**(21), 3430.
29 T. Kim, T. T. Tung, T. Lee, J. Kim and K. S. Suh, *Chem.–Asian J.*, 2010, **5**, 256.
30 Y. Li, G. Li, X. Wang, Z. Zhu, H. Ma, T. Zhang and J. Jin, *Chem. Commun.*, 2012, **48**, 8222.